Unusual Doping Dependence of the Electronic Structure and Coexistence of Spin-Density-Wave and Superconductor Phases in Single Crystalline $Sr_{1-x}K_xFe_2As_2$

Y. Zhang,[1] J. Wei,[1] H. W. Ou,[1] J. F. Zhao,[1] B. Zhou,[1] F. Chen,[1] M. Xu,[1] C. He,[1] G. Wu,[2] H. Chen,[2] M. Arita,[3] K. Shimada,[3] H. Namatame,[3] M. Taniguchi,[3] X. H. Chen,[2] and D. L. Feng[1,*]

[1]*Department of Physics, Surface Physics Laboratory (National Key Laboratory), and Advanced Materials Laboratory, Fudan University, Shanghai 200433, People's Republic of China*

[2]*Hefei National Laboratory for Physical Sciences at Microscale and Department of Physics, University of Science and Technology of China, Hefei, Anhui 230026, People's Republic of China*

[3]*Hiroshima Synchrotron Radiation Center and Graduate School of Science, Hiroshima University, Hiroshima 739-8526, Japan*

(Received 24 August 2008; published 26 March 2009)

The nature of the spin-density wave (SDW) and its relation with superconductivity are crucial issues in the newly discovered iron-pnictide superconductors. Particularly, it is unclear whether the superconducting phase and SDW are truly exclusive from each other. We here report splittings of the band structures in $Sr_{1-x}K_xFe_2As_2$ ($x = 0$, 0.1, 0.18), and their unusual doping dependence. Our data on single crystalline samples prove that the SDW and superconductivity could coexist in iron pnictides.

DOI: 10.1103/PhysRevLett.102.127003 PACS numbers: 74.25.Jb, 71.20.−b, 74.70.−b, 79.60.−i

Both the cuprate and the iron-pnictide high-temperature superconductors are in the vicinity of certain magnetic order [1]. For the cuprate, the antiferromagnetic spin fluctuations might likely facilitate the *d*-wave pairing, which makes the nature of the spin-density wave (SDW) in the iron pnictides and its relation with the superconductivity central issues. Recently, we have found that certain band splittings are associated with the SDW formation in $BaFe_2As_2$ [2]. This is beyond the prediction of all the existing band structure calculations. The detailed behaviors of the splitting thus need to be uncovered to further understand its cause.

The band splitting observed at the onset of the SDW does not necessarily open an energy gap at the Fermi energy (E_F), which leaves room for superconductivity. Early resistivity data have indirectly suggested that the SDW and superconductivity could coexist in $LaO_{1-\delta}F_\delta FeAs$ [3], $SmO_{1-\delta}F_\delta FeAs$ [4]. However, more recent neutron diffraction, muon spin relaxation (μSR), and Mössbauer spectroscopy indicate that they are exclusive from each other for $CeO_{1-\delta}F_\delta FeAs$ [5] and $LaO_{1-\delta}F_\delta FeAs$ [6]. On the other hand, recent experiments on polycrystalline $Ba_{1-x}K_xFe_2As_2$ indicate that the SDW and superconductivity could coexist for $x \in (0.1, 0.4)$ based on combined transport, x-ray and neutron diffraction data [7]. If possible phase segregation can be ruled out, this would allude to a new ground state in $Ba_{1-x}K_xFe_2As_2$, where Cooper pairs are formed on a SDW background. This resembles the Hg-based five-layer cuprate, where antiferromagnetic order coexists with the superconductivity uniformly within single CuO_2 plane [8].

In this Letter, we report angle resolved photoemission spectroscopy (ARPES) measurements of $Sr_{1-x}K_xFe_2As_2$ single crystals. $SrFe_2As_2$ has the highest known SDW transition temperature (T_S) of about 205 K in iron pnictides [9]. We show with systematic data that the band splitting is a sign of the SDW on the electronic structure, and it occurs in $Sr_{1-x}K_xFe_2As_2$, with descending onset temperatures and amplitudes for $x = 0$, 0.1, 0.18. Since $Sr_{0.82}K_{0.18}Fe_2As_2$ has a superconducting transition temperature (T_c) of 25 K, we prove that superconductivity and the SDW indeed coexist even for single crystals, which sheds new light on the interplay of superconductivity and magnetism in iron-pnictide superconductors. Moreover, the unusual doping dependence of the splitting further highlights its complexity and correlated nature, providing new clues for sorting out its mechanism.

The $Sr_{1-x}K_xFe_2As_2$ ($x = 0$, 0.1, 0.18) single crystals were synthesized with the tin flux method [10], where the doping x is determined through energy-dispersive x-ray (EDX) analysis. The resistivity data in Fig. 1 indicate

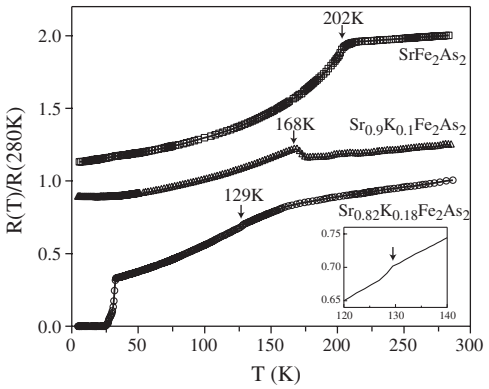

FIG. 1. Relative resistance (with respect to the resistance at 280 K) of $Sr_{1-x}K_xFe_2As_2$ ($x = 0$, 0.1, 0.18) vs temperature. The $x = 0$ and $x = 0.1$ curves are shifted up by 1 and 0.25, respectively. The inset is an enlargement of the $x = 0.18$ data around 130 K.

that the undoped compound ($x = 0$) enters the SDW state at about 202 K, and there is an anomaly at 168 K for $x = 0.1$. The $x = 0.18$ compound reaches the zero resistance superconducting phase at about 25 K with a transition width of 5 K (10%–90%), and there is a small sharp drop of resistivity at about 129 K, as enlarged in the inset. For the $x = 0.18$ sample, an EDX survey with high sampling density across the entire 0.8×0.8 mm^2 surface area shows that it is very homogeneous, and the standard deviation of its K doping level is about 0.017 (note the instrumentation accuracy is 0.01). Therefore, the entire sample is thus well within the superconducting phase [11]. The data presented were taken with 24 eV photons from beam line 5-4 of the Stanford synchrotron radiation laboratory (SSRL) and beam line 9 of the Hiroshima synchrotron radiation center. Other photon energies have been exploited to ensure the measured electronic structure to be intrinsic, and reflecting the bulk behavior (e.g., using 7.65 eV low energy photons). With Scienta R4000 electron analyzers, the overall energy resolution is 10 meV, and angular resolution is 0.3°. The samples were cleaved *in situ*, and measured under ultrahigh vacuum of 3×10^{-11} torr. The sample aging effects are negligible during the experiment, indicative of a stable surface.

The normal state band structure of $SrFe_2As_2$ is presented through the photoemission intensity and its second derivative with respect to energy along the Γ–M cut [Figs. 2(a) and 2(b)]. Three bands (named as α, β, and γ band, respectively) could be identified to cross E_F, with the assistance from the momentum distribution curves (MDC's) in Fig. 2(c). Near M, the α and β bands appear quite flat and degenerate, and do not cross E_F. There are thus two hole-type Fermi surfaces around Γ, and one electron-type Fermi surface around M [Fig. 2(d)], as predicted by the band structure calculations [12–18]. In the SDW state, the data along the same cut are measured for comparison [Figs. 2(e)–2(g)]. Three Fermi crossings (k_F's) could be resolved near Γ. The α band is closer to Γ, giving a smaller hole pocket than the normal state one. The β band is pushed away from Γ, and splits into two bands, which are assigned as β_1 and β_2, respectively. Around M, the normal-state flat feature splits into three bands. Correspondingly, the β_1 band is pushed down by about 60 meV; the β_2 band is pushed up to cross E_F; and the α

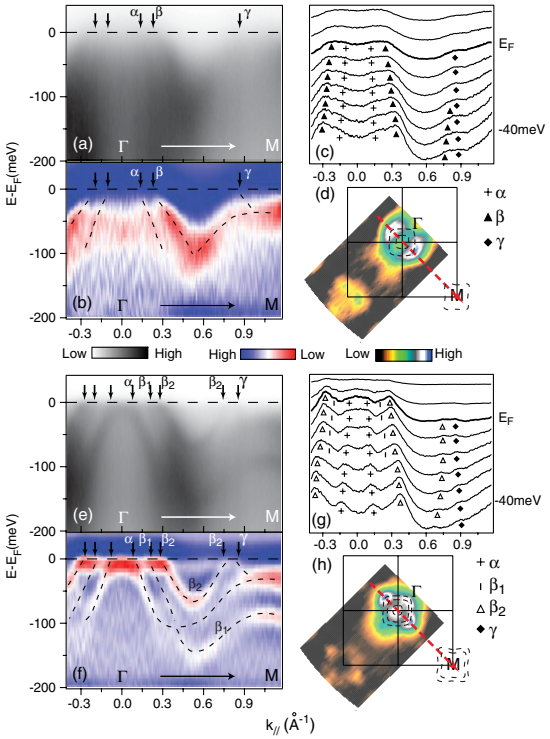

FIG. 2 (color online). Electronic structure of $SrFe_2As_2$. (a) Photoemission intensity along the Γ–M cut as indicated in panel (d). (b) The second derivative of the data in panel (a). (c) The MDC's near E_F for the data in panel (a). (d) Photoemission intensity map at E_F in the Brillouin zone, where the measured Fermi surface sheets are shown by dashed curves. Only one set of Fermi surface around M is plotted for a clearer view. Data were taken at 230 K. (e),(f),(g),(h) are the same as in panel (a),(b),(c),(d), respectively, but taken at 10 K.

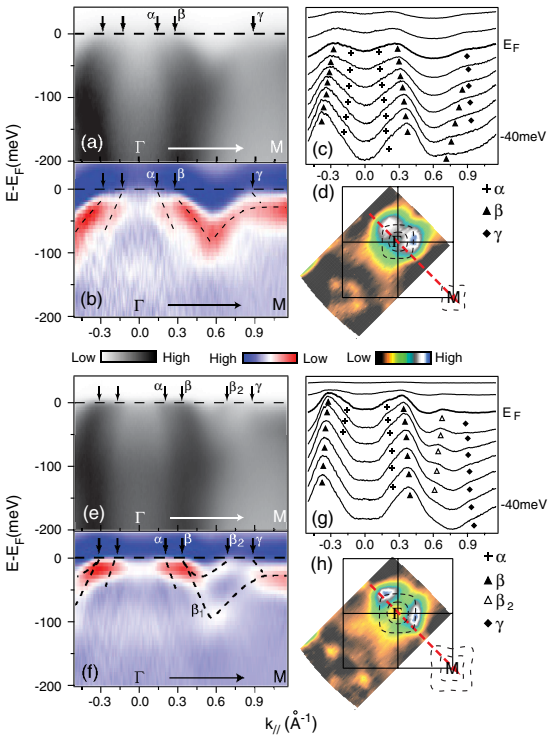

FIG. 3 (color online). Electronic structure of $Sr_{0.82}K_{0.18}Fe_2As_2$. (a) Photoemission intensity along the Γ–M cut as shown in panel (d). (b) The second derivative of the data in panel (a). (c) The MDC's near E_F for the data in panel (a). (d) Photoemission intensity map at E_F in the Brillouin zone. Data were taken at 150 K. (e),(f),(g),(h) are the same as in panel (a),(b),(c),(d), respectively, but taken at 10 K. The dispersion of the α band in panels (b) and (f) is determined from the MDC analysis as shown in panels (c) and (g), respectively.

band is more or less unaffected. Moreover, the electronlike nature of the γ pocket could be better resolved in Figs. 2(f) and 2(g) than in the normal state, and its k_F does not show any noticeable movement. As shown in Fig. 2(h), the SDW state has two more hole pockets than the normal state, one around Γ and one around M. Fermi surface folding in the SDW state was not observed.

The electronic structure in the hole-doped $Sr_{0.82}K_{0.18}Fe_2As_2$ superconductor is illustrated in Fig. 3. At high temperatures [Figs. 3(a)–3(d)], it is similar to that in the normal state of $SrFe_2As_2$. As expected, the two hole pockets around Γ grow larger, and the electron pocket around M slightly shrinks with hole doping. At 10 K, the most prominent difference occurs midway in the Γ–M cut, where two features are observed in Figs. 3(f) and 3(g), one of which (the β_2 band) crosses E_F, and gives an additional large hole pocket around M at 10 K in Fig. 3(h).

Detailed temperature evolution of the splitting in $Sr_{1-x}K_xFe_2As_2$ is shown through the second derivative of the photoemission intensity in Fig. 4. For $SrFe_2As_2$, although no obvious temperature dependence is observed for the α band within the experimental resolution, the splitting of the β band occurs abruptly between 200 K and 195 K in Figs. 4(b) and 4(c), and develops rapidly with the decreasing temperatures. At the lowest temperature, the hybridization of the α and β_1 bands could also be resolved clearly when they cross. However, the bands are named as if they were not crossing for simplicity.

For $x = 0.1$ and $x = 0.18$, band splittings occur very abruptly as well. The onset temperatures are estimated to be 165 ± 5 K and 135 ± 5 K for $x = 0.1$ and 0.18, respectively, as shown in Figs. 4(h)–4(l) and 4(n)–4(s). The splitting is momentum dependent in all cases. By extracting the largest splitting between the β_1 and β_2 bands at the k_F of β_2 (which are close to their splittings at M by fit), one gets 120 meV, 85 meV, and 60 meV for $x = 0$, 0.1, and 0.18, respectively, consistent with the decreasing onset temperatures of the splitting. As a comparison, the splitting around Γ is just about 50 meV for $x = 0$. We note for $BaFe_2As_2$, $T_S = 138$ K, and the maximal splitting is about 75 meV near M [2]; both are close to the $Sr_{0.9}K_{0.1}Fe_2As_2$ case. Furthermore, all systems show similar spectral characters when the splittings are the most obvious. For example, the temperature evolutions of photoemission spectra at $k = 0.6$ Å^{-1} are quite similar in Figs. 4(g), 4(m), and 4(t) for $x = 0$, 0.1, 0.18, respectively.

The observed band splittings always occur almost exactly at the resistivity anomaly temperatures, which are known to be the bulk SDW transition temperatures for the undoped systems. This correlation also indicates that the measured electronic structure reflects the bulk properties. Similar to $BaFe_2As_2$ [2], such a splitting on the order of several k_BT_S and its temperature dependence cannot be explained by factors such as structure transition or spin orbital coupling. On the other hand, although detailed theoretical understanding is yet to be achieved, it might be explained by the exchange splitting associated with the SDW formation. The exchange splittings in SDW materials have been observed before [19,20]. In fact, because more electrons will be relocated into the bands that are pushed downward than those relocated in the bands split upward, the electronic energy of the system can be saved

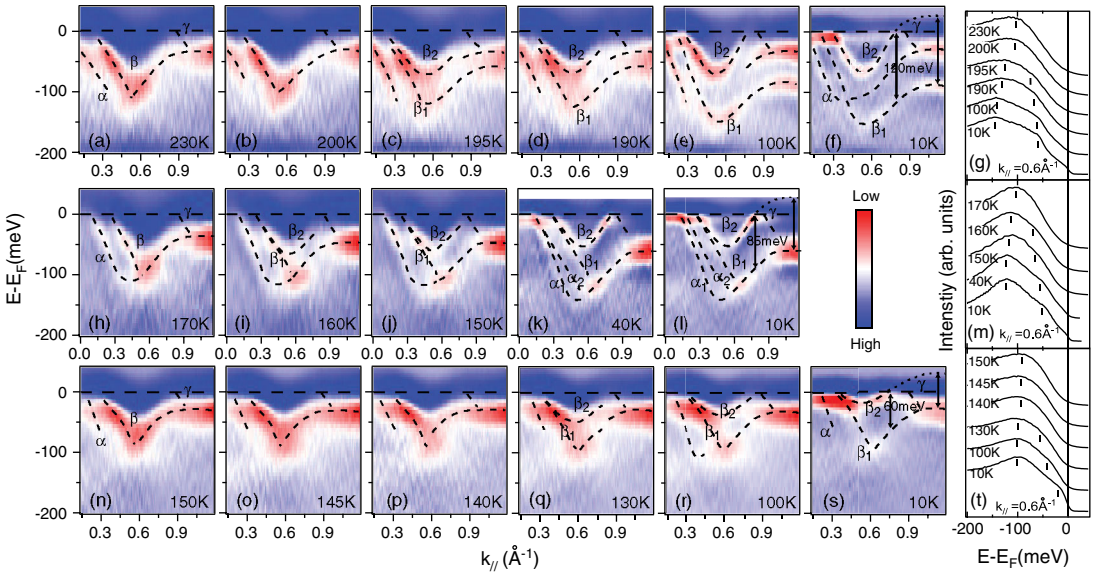

FIG. 4 (color online). Temperature dependence of the bands (dashed lines) along Γ–M as determined by the minima of the second derivative of photoemission intensity with respect to energy or MDC peaks for $Sr_{1-x}K_xFe_2AS_2$ with (a)–(f) $x = 0$, (h)–(l) $x = 0.1$, and (n)–(s) $x = 0.18$ at the labeled temperatures. Note the minimum of the second derivative represents a peak, thus the lower part (red or white color) represents the band. (g), (m), and (t) are the temperature evolution of energy distribution curves at $k = 0.6$ Å^{-1} for $x = 0$, 0.1 and 0.18, respectively. Note the momentum window is slightly wider for $x = 0.1$ data.

through such a splitting, and thus it can be responsible for the SDW. Consistently, the band splitting is of the same scale as the exchange interactions between the nearest and next-nearest neighbor local moments estimated from band calculations [2,21]. In this regard, the observed systematics, such as the correlations among doping, onset temperature, and splitting amplitude, and similar spectral characters indicate that the observed splitting is a sign of the SDW, and thus there are coexisting SDW and superconductivity in $Sr_{0.82}K_{0.18}Fe_2As_2$. We emphasize this is not due to some inhomogeneity, because in addition to the EDX results, the drastic doping dependence of the splitting amplitude and onset temperature further ensure that the K concentration is homogeneous here. Since if there were domains with different dopings, we would have observed many sets of bands, and a broad onset temperature range.

The paramagnetic state electronic structures of various iron pnictides qualitatively resemble each other [2,22–25], regardless of their chemical environment or doping, as exemplified here for $Sr_{1-x}K_xFe_2As_2$. The doping behavior is consistent with a rigid-band picture. Nevertheless in the SDW state, the behaviors of their splitting is different. Figure 4 highlights the unusual doping dependence. Taking the splitting at M as an example, the shifts of both the β_1 and β_2 bands are equally strong from the normal-state position for $x = 0$; for $x = 0.1$, β_2 shifts much more than β_1; for $x = 0.18$, only β_2 shows obvious shift. While for $BaFe_2As_2$, all bands shift strongly at M [2]. Moreover, the electron Fermi pocket around M splits into one large electron pocket and one small electron pocket in $BaFe_2As_2$; but for $SrFe_2As_2$, the size of the γ pocket does not change noticeably, indicating a negligible splitting. These nontrivial findings unveil the correlated or non-rigid-band aspect of the splitting. Its behavior appears quite different from the conventional exchange splitting observed in various ferromagnets. Furthermore, when entering the SDW state, both the density of states at E_F and the quasiparticle scattering would be affected by these electronic structure changes drastically. Their different temperature dependencies may conspire to cause the drastically different transport behaviors in Fig. 1, reiterating the correlated nature of the splitting.

The coexistence of the SDW and superconductivity has profound consequences on the nature of the superconductivity. Firstly, it suggests that the superconducting gap might open at one more (β_2) Fermi surface sheet here than in the $Ba_{0.6}K_{0.4}Fe_2As_2$ reported earlier [23,24]. Secondly, taking a split majority band as an example, its electron spins are in phase with the SDW order. In the singlet pairing channel, a Cooper pair made of electrons at $\pm k_F$ will have its spin-up and spin-down electrons mainly situated in the spin-up and spin-down sites of the SDW, respectively; and vice versa for the minority band. This gives a novel ground state that is not known before. Thirdly, how the SDW competes with the superconductivity in iron pnictides would be another interesting issue. On the other hand, the magnetic fluctuations related to the SDW might even play a constructive role in superconductivity as in cuprates. We leave these issues to future detailed studies.

To summarize, we show that the behaviors of the band splitting differ prominently in various iron pnictides. Our results provide new clues for understanding the band splitting and SDW in iron pnictides. Particularly, we demonstrate in the single crystalline $Sr_{0.82}K_{0.18}Fe_2As_2$ that the SDW and superconductivity could coexist, revealing a new kind of ground state, which would help understand the relationship between the SDW and superconductivity in iron pnictides.

We thank Dr. W. Bao for inspiring discussions, and Dr. D. H. Lu and Dr. R. G. Moore for their experimental assistance at SSRL. This work was supported by the NSFC, MOE, MOST (National Basic Research Program No. 2006CB921300), and STCSM of China. SSRL is operated by the US DOE Office of Basic Energy Science.

*dlfeng@fudan.edu.cn

[1] C. de la Cruz *et al.*, Nature (London) **453**, 899 (2008).
[2] L. X. Yang *et al.*, arXiv:0806.2627v2.
[3] Y. Kamihara *et al.*, J. Am. Chem. Soc. **130**, 3296 (2008).
[4] R. H. Liu *et al.*, Phys. Rev. Lett. **101**, 087001 (2008).
[5] J. Zhao *et al.*, Nature Mater., **7**, 953 (2008).
[6] H. Luetkens *et al.*, arXiv:0806.3533.
[7] H. Chen *et al.*, Europhys. Lett. **85**, 17 006 (2009).
[8] H. Mukuda *et al.*, Phys. Rev. Lett. **96**, 087001 (2006).
[9] C. Krellner *et al.*, Phys. Rev. B **78**, 100504(R) (2008).
[10] J. Q. Yan *et al.*, Phys. Rev. B **78**, 024516 (2008).
[11] H. Q. Luo *et al.*, Supercond. Sci. Technol. **21**, 125014 (2008).
[12] D. J. Singh and M. H. Du, Phys. Rev. Lett. **100**, 237003 (2008).
[13] G. Xu, W. Ming, Y. Yao, X. Dai, and Z. Fang, Europhys. Lett. **82**, 67 002 (2008).
[14] I. I. Mazin, D. J. Singh, M. D. Johannes, and M. H. Du, Phys. Rev. Lett. **101**, 057003 (2008).
[15] C. Cao, P. J. Hirschfeld, and H.-P. Cheng, Phys. Rev. B **77**, 220506(R) (2008).
[16] F. Ma and Z. Y. Lu, Phys. Rev. B **78**, 033111 (2008).
[17] F. Ma, Z. Y. Lu and T. Xiang, arXiv:0806.3526.
[18] J. Dong *et al.*, Europhys. Lett. **83**, 27 006 (2008).
[19] F. J. Himpsel, Phys. Rev. Lett. **67**, 2363 (1991).
[20] L. W. Bos and D. W. Lynch, Phys. Rev. B **2**, 4567 (1970).
[21] F. Ma, Z. Y. Lu, and T. Xiang, Phys. Rev. B **78**, 224517 (2008).
[22] D. H. Lu *et al.*, Nature (London) **455**, 81 (2008).
[23] L. Zhao *et al.*, Chin. Phys. Lett. **25**, 4402 (2008).
[24] H. Ding *et al.*, Europhys. Lett. **83**, 47 001 (2008).
[25] C. Liu *et al.*, Phys. Rev. Lett. **101**, 177005 (2008).